Clinical Cancer Research

KRAS Mutation and Consensus Molecular Subtypes 2 and 3 Are Independently Associated with Reduced Immune Infiltration and Reactivity in Colorectal Cancer

Neeraj Lal[1], Brian S. White[2], Ghaleb Goussous[1], Oliver Pickles[1], Mike J. Mason[2], Andrew D. Beggs[3], Philippe Taniere[4], Benjamin E. Willcox[1], Justin Guinney[2], and Gary W. Middleton[1,4]

Abstract

Purpose: *KRAS* mutation is a common canonical mutation in colorectal cancer, found at differing frequencies in all consensus molecular subtypes (CMS). The independent immunobiological impacts of RAS mutation and CMS are unknown. Thus, we explored the immunobiological effects of *KRAS* mutation across the CMS spectrum.

Experimental Design: Expression analysis of immune genes/signatures was performed using The Cancer Genome Atlas (TCGA) RNA-seq and the KFSYSCC microarray datasets. Multivariate analysis included *KRAS* status, CMS, tumor location, MSI status, and neoantigen load. Protein expression of STAT1, HLA-class II, and CXCL10 was analyzed by digital IHC.

Results: The Th1-centric co-ordinate immune response cluster (CIRC) was significantly, albeit modestly, reduced in *KRAS*-mutant colorectal cancer in both datasets. Cytotoxic T cells, neutrophils, and the IFNγ pathway were suppressed in *KRAS*-mutant samples. The expressions of STAT1 and CXCL10 were reduced at the mRNA and protein levels. In multivariate analysis, *KRAS* mutation, CMS2, and CMS3 were independently predictive of reduced CIRC expression. Immune response was heterogeneous across *KRAS*-mutant colorectal cancer: *KRAS*-mutant CMS2 samples have the lowest CIRC expression, reduced expression of the IFNγ pathway, *STAT1* and *CXCL10*, and reduced infiltration of cytotoxic cells and neutrophils relative to CMS1 and CMS4 and to *KRAS* wild-type CMS2 samples in the TCGA. These trends held in the KFSYSCC dataset.

Conclusions: *KRAS* mutation is associated with suppressed Th1/cytotoxic immunity in colorectal cancer, the extent of the effect being modulated by CMS subtype. These results add a novel immunobiological dimension to the biological heterogeneity of colorectal cancer. *Clin Cancer Res; 24(1); 224–33. ©2017 AACR.*

Introduction

Galon and colleagues first demonstrated the positive prognostic impact of tumor-infiltrating lymphocytes (TIL) in colorectal cancer (1). The strength of Th type 1 (Th1) adaptive immunity was shown to be a strong prognostic factor. Th1 cells have an essential role in initiating and maintaining an effective $CD8^+$ cytotoxic T-cell response (2–4), in the recruitment of $CD8^+$ cells to the tumor bed (5) and in directly mediating immunologic tumor cell death (6). Th1 cells recognize antigen in association with MHC-II molecules. They secrete the inflammatory cytokine IFNγ, which provokes class II upregulation on tumor cells. The majority of immunogenic neoepitopes are class II restricted (7). Tumor cells evade cytotoxic immune responses by expressing the programmed death-ligand 1 (PD-L1) that activates the PD-1 negative feedback pathway (8). This checkpoint may be inhibited using anti–PD-1 or anti–PD-L1 antibodies that block interactions between the PD-1 receptor and its ligand PD-L1. However, the strategy has only been efficacious in microsatellite unstable (MSI-high) colorectal cancer (9), that is, those having a high neoantigen burden that can stimulate microenvironmental immunological reactivity (10). Class II expression on cancer cells is clearly important in the efficacy of checkpoint blockage. Indeed, cancer cell MHC-II–negative melanoma patients have lower response rates, PFS, and OS when treated with PD-1/PD-L1 blockade relative to class II-positive patients (11). Furthermore, *in vitro* PD-L1 blockade enhances Th1-mediated cytotoxicity only against cells that express high class II (12). Hence, an effective immune response is critically dependent on neoantigen presentation by MHC-II molecules.

The upregulation of MHC-II molecules via the IFNγ pathway is dependent on the STAT1 and CIITA proteins: extracellular IFNγ induces and activates STAT1, which activates transcription of CIITA. CIITA is the master transcriptional activator of MHC-II

[1]Institute of Immunology and Immunotherapy, University of Birmingham, Birmingham, United Kingdom. [2]Computational Oncology, Sage Bionetworks, Seattle, USA. [3]Institute of Cancer and Genomic Sciences, University of Birmingham, Birmingham, United Kingdom. [4]University Hospitals Birmingham NHS Foundation Trust, Birmingham, United Kingdom.

Note: Supplementary data for this article are available at Clinical Cancer Research Online (http://clincancerres.aacrjournals.org/).

N. Lal and B.S. White contributed equally to this article.

J. Guinney and G.W. Middleton are co-senior authors of this article.

Corresponding Author: Gary W. Middleton, University of Birmingham, Vincent Drive, Birmingham B15 2TT, United Kingdom. Phone: 121-415-8237; Fax: 121-371-3590; E-mail: g.middleton@bham.ac.uk

doi: 10.1158/1078-0432.CCR-17-1090

Translational Relevance

Understanding how mutational and transcriptional differences mold the immune contexture in cancer is key to accurate immunobiological stratification. We analyze how KRAS mutation shapes the immune microenvironment of colorectal cancer in the context of the consensus molecular subtypes (CMS). We show that KRAS mutation is associated with modest suppression of Th1 cell and cytotoxic cell immunity independently of mismatch repair status, tumor location, neoantigen load, and transcriptional subtype, but also show that the cumulative effect is dependent upon the CMS in which the mutation is found. Immunity in KRAS-mutant CMS2 is more suppressed than CMS1 and CMS4 as well as in comparison with KRAS wild-type CMS2. Our findings refine stratification factors for immunotherapy trial entry in colorectal cancer and suggest potential immunotherapeutic strategies to test in KRAS-mutant patients. Variation in the immune status of RAS-mutant colorectal cancer according to its transcriptional context might underlie part of the heterogeneity of response to molecularly stratified medicines.

molecules. STAT1-deficient cells show no induction of *CIITA* mRNA despite IFNγ stimulation (13) and STAT1-deficient cancer cells progress rapidly due to the evasion of adaptive immunity (14). Class I–positive but class II–negative mammary adenocarcinoma cells grew rapidly in immunocompetent mice, but were rejected when these cells were transfected with CIITA. Rejection correlated with induction of class II expression and was mediated by both $CD4^+$ and $CD8^+$ cells. STAT1 deficiency also severely impairs the induction of CXCL10, another STAT1 target gene. CXCL10 maintains the Th1 phenotype (15), and the decreased accumulation of Th1 cells in STAT1-deficient mice is related to reduced levels of CXCL10 (16).

KRAS mutation is the commonest canonical gain-of-function mutation in colorectal cancer, and earlier functional studies clearly demonstrated that mutant RAS reduces both STAT1 and class II expression. Using different cell line models (including HCT116 and clones thereof with deleted mutant KRAS, and intestinal epithelial cells with inducible mutant RAS), Klampfer and colleagues demonstrated that mutant RAS downregulates both constitutive and IFNγ-inducible STAT1 mRNA and protein and reduces STAT1 transcriptional activity and the expression of many IFNγ target genes, including class II (17, 18). Maudsley and colleagues showed that mutant KRAS resulted in loss of class II inducibility upon IFNγ treatment (without inhibiting class I expression), significantly reduced the ability of these cells to stimulate allogeneic T cells, and reduced the IFNγ secretion of the costimulated cells (19). They suggested that this RAS-mediated class II downregulation interrupted an amplification loop whereby Th1 cells are stimulated to produce IFNγ that would then stimulate further cancer cell class II expression.

These isolated cell line experiments suggest a role for STAT1 and its target genes in RAS-mutant colorectal cancer, but fail to replicate the complexities of the intact tumoral microenvironment. Hence, guided by these preclinical studies, we asked whether RAS-mutant colorectal cancer was associated with reduced expression of STAT1, CIITA, and CXCL10, as well as that of a number of associated signatures of immune reactivity, in human colorectal cancer tumor tissues. We have previously demonstrated using transcriptional analysis of bulk tumors that RAS-mutant colorectal cancer is associated with lower expression of a Th1-centric immune metagene that we termed the Co-ordinate Immune Response Cluster (CIRC; ref. 20). This metagene includes *STAT1*, *CXCL10*, nine separate class II genes, and the Th1 transcription factor T-bet (*TBX21*). We have also previously described a second immunological stratifier, the colorectal cancer "consensus molecular subtypes" (CMS; ref. 21). These subtypes include a "mesenchymal" group (CMS4) that is enriched for MSS tumors and yet is characterized by appreciable immune infiltration, intermediate between that of the MSI-enriched subtype (CMS1) and of the "canonical" (CMS2) and "metabolic" (CMS3) subtypes. RAS mutations occur in all of these CMS subtypes (albeit with differing proportions), and thus, RAS mutations in colorectal cancer occur in different transcriptional contexts with heterogeneous biology. In particular, RAS mutations are present in both mismatch repair–deficient and proficient cancers. To determine whether these two stratifiers are independent, we dissected the various innate and adaptive immune components of the CIRC in the context of CMS and KRAS mutation status using transcriptional analysis of two large independent datasets and digital IHC analysis of compartment-specific protein expression.

We demonstrate that CMS is more strongly associated with reduced anticancer immunity in colorectal cancer than RAS mutation, with both CMS2 and CMS3 being immunosuppressed relative to CMS1 and CMS4. Nevertheless, we find that the modest RAS mutation association is significant and independent of expression subtype. The cumulative effect on immunity is dependent upon the CMS context of RAS mutation, with RAS-mutant CMS2 being particularly immunosuppressed.

Materials and Methods

CMS analysis

Statistical analyses of The Cancer Genome Atlas (TCGA) and KFSYSCC expression data were performed in R (https://www.r-project.org/). To summarize the expression of a gene set [i.e., CIRC, immune subpopulations (22), and Hallmark gene sets (23)], we condensed the expression of the multiple genes in the set into a single gene set enrichment value using gene set variation analysis (24). Two-tailed nonparametric Wilcoxon rank sum tests, two-tailed *t* tests, two-tailed Fisher tests, and one-tailed *F* tests were applied, as indicated. Relative enrichments or expression between two populations are summarized by the Hodges–Lehmann estimator of the difference between those populations, for example, the median of all pairwise differences between CIRC enrichment in a *KRAS* WT sample and a *KRAS* MT sample. Ninety-five percent confidence intervals in this estimator were calculated using the method of Bauer (25). Multivariate analyses were performed using the forestmodel R package, with linear model CIRC ~ KRAS + CMS + site + status + neoantigens and where CIRC is the gene set enrichment for the immune signature, site indicates tumor location as left, right, or rectum, KRAS indicates mutation status WT or MT, CMS indicates subtype, status indicates MSI or MSS, and neoantigens is a continuous value indicating the (log-transformed) number of neoantigens. To assess potential synergy between the main effects corresponding to CMS subtype (CMS) and *KRAS* mutation status (KRAS), we used ANOVA to compare

linear models with and without the interaction effect (CMS: KRAS), i.e., CIRC ~ CMS + KRAS versus CIRC ~ CMS + KRAS + CMS:KRAS. Samples that did not correspond to one of the four CMS groups (i.e., "unlabeled") were excluded from any analysis that include CMS. Expression datasets, as well as clinical annotations, CMS labels, neoantigen predictions (obtained from The Cancer Immune Atlas; ref. 26), and gene set definitions, are available on the Synapse data commons platform (ref. 27 and https://www.synapse.org) under Synapse ID syn8533552. Source code to perform all genomic analyses and to generate the respective figures is available at https://github.com/Sage-Bionetworks/crc-cms-kras. Additional detail is provided in Supplementary Methods.

IHC analysis

Samples for IHC from patients undergoing resection of primary colorectal cancer were obtained from the completed CRUK Stratified Medicine Programme One pilot study and colorectal cancer patients from the Queen Elizabeth Hospital (Birmingham, United Kingdom). Samples were collected under ethical approval HBRC 14-205 (Sponsor: University of Birmingham). All patients had provided informed written consent for the use of their tissue, and studies were conducted in accordance with the Declaration of Helsinki. The cohort comprised 28 RAS G12D/G13D mutants (24.3%), 38 RAS non-G12D/G13D mutants (33.0%), and 49 RAS wild types (42.65%) for a total of 115. Suitable formalin-fixed, paraffin-embedded (FFPE) blocks were retrieved and processed at the HBRC biobank, University of Birmingham. Microsatellite status was assessed by extracting total DNA from FFPE tumor scrolls by fragment analysis (Supplementary Methods). Seven tumors (6.09%) were MSI-high, of which 3 were RAS mutant.

IHC was performed using a Leica BOND-MAX autostainer. For STAT1, an antibody that had undergone robust validation was selected (Cell Signaling Technology clone D1K9Y). For class II HLA (Abcam clone CR3/43) and CXCL10 (Novus Biologicals clone 6D4), in-house validation was performed as described in Supplementary Methods.

Staining conditions and concentrations were iteratively optimized in conjunction with a histopathologist (P. Taniere): STAT1: 1:500, 20-minute incubation, class II HLA: 1:100, 20 minutes, CXCL10: 1:50, 20 minutes. Slides were scanned at ×40 magnification using a Leica SCN400 slide scanner and digitally analyzed using Definiens Tissue Studio software. Analysis algorithms were created and optimized for each marker. Regions of interest were created in the tumor regions of each slide. All tumors were digitally segmented into tumor epithelium and stroma regions using trained segmentation algorithms (Supplementary Fig. S1A and S1B). Depending on the marker, staining was quantified on a per cell basis or on an area basis (Supplementary Fig. S1C and S1D). Percentages of cells or pixels with high, medium, low, or no immunoreactivity were quantified in each region. This produced either histologic scores for cell-based scoring, or percentile scores for pixel-based scoring, which are functions of the number and intensity of immunoreactive cells or pixels in the scanned specimens respectively [1 × (% cells/pixels with low staining) + 2 × (% cells/pixels with medium staining) + 3 × (% cells/pixels with high staining) = score out of 300]. Thresholds for negative/low, low/medium, and medium/high were set for each antibody in conjunction with a pathologist to maximize the dynamic range of results between samples and to reduce false-positive results. Hematoxylin thresholds (the staining intensities at which hematoxylin was recognized) were set individually and differed for each antibody due to differences in DAB staining. Hematoxylin thresholds were set to ensure accurate identification of individual cells. After analysis, segmentation was manually validated for each slide.

IHC results were analyzed using Excel (Microsoft Corp.) and Minitab (Minitab, Inc.). The normality of the distribution of histologic scores in each group (*RAS* mutant or *RAS* wild type) was determined by performing the Anderson–Darling test. All data were nonparametrically distributed. Therefore, for one-by-one comparisons, Mann–Whitney *U* tests were performed for significance testing. In addition, for STAT1 and CXCL10, staining for each case was grouped into low and high using H-score thresholds of both 100 and 200. For class II HLA, cases were grouped into negative (0%–5% staining), low (5%–50% staining), and high (>50% staining) as described by Lovig and colleagues (Supplementary Fig. S2F–S2H; ref. 28). χ^2 tests were performed to investigate significance between the RAS-mutant and wild-type groups. $P < 0.05$ was considered statistically significant.

Results

Immune subpopulations are suppressed in *KRAS* MT colorectal cancer

In our previous work, we demonstrated that RAS-mutant colorectal cancer had lower expression of the CIRC, a metagene that integrates 28 genes involved in innate and adaptive immunity (20). The CIRC was defined using 195 microarray colorectal cancer samples, of which 190 have also been subjected to RNA sequencing (RNA-seq) as part of an extended TCGA study. We analyzed this full dataset ($n = 344$) to validate our original findings on the orthogonal RNA-seq platform: consistent with those previous results, the analysis showed a significant reduction in the expression of the CIRC metagene in *KRAS* mutant (MT) relative to wild type (WT) samples (Supplementary Fig. S3A; two-tailed Wilcoxon rank sum $P = 2.4 \times 10^{-3}$). We additionally validated these results in the independent KFSYSCC (29) dataset ($n = 290$) of fresh-frozen colorectal cancer samples (Supplementary Fig. S3B; two-tailed Wilcoxon rank sum $P = 4.4 \times 10^{-3}$).

The CIRC signature was previously defined by performing an unsupervised hierarchical clustering of TCGA patients based on 61 highly curated, immune response–related genes. The genes comprising the signature were selected on the basis of their strong coordinated regulation across patient subgroups (20). The CIRC is enriched for Th1-associated genes, as well as genes encoding chemokines, adhesion molecules, MHC class II molecules, and immune checkpoints. Therefore, to dissect the specific immune subpopulations differentially recruited to *KRAS* MT tumors, we examined the effect of *KRAS* mutation on expression of each of seven immune cell types [neutrophils, and immature dendritic (iDC), B, T, Th1, Th2, and cytotoxic cells (22)]. Despite having few genes in common (Supplementary Fig. S4), all immune subpopulations except Th2 cells were highly correlated with the CIRC in both datasets (Pearson correlation $r \geq 0.42$; $P \leq 6.4 \times 10^{-14}$; Supplementary Fig. S5). Cytotoxic ($r \geq 0.85$; $P \leq 4.3 \times 10^{-82}$), T ($r \geq 0.73$; $P \leq 2.7 \times 10^{-50}$), and, as expected, Th1 ($r \geq 0.71$; $P \leq 3.2 \times 10^{-45}$) cells were most highly correlated with the CIRC in both datasets. *KRAS* mutation is associated with reduced cytotoxic cell (Fig. 1A; TCGA: two-tailed Wilcoxon rank sum $P = 0.04$; KFSYSCC: $P = 0.02$) and neutrophil (TCGA: $P = 9.7 \times 10^{-3}$; KFSYSCC: $P = 5.3 \times 10^{-3}$) infiltration. Th1 cells themselves

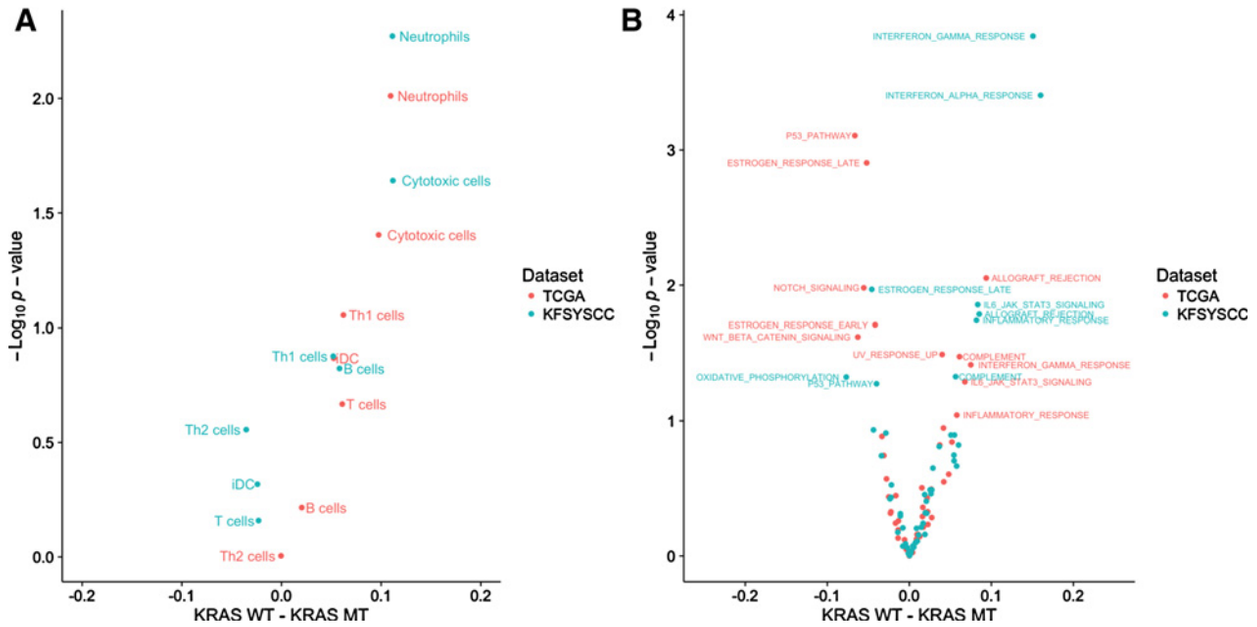

Figure 1.

KRAS mutation is associated with reduced immune infiltration and downregulation of immune pathways. **A,** Volcano plot showing enrichment (*x*-axis) of immune cell subpopulations in *KRAS* WT relative to *KRAS* MT tumors, with associated *P* values (*y*-axis) across TCGA (red) and KFSYSCC (blue) datasets. Relative enrichment is the Hodges–Lehmann estimator of the difference between the *KRAS* WT and *KRAS* MT populations, that is, the median of all pairwise differences between the enrichment in an indicated immune subpopulation in a *KRAS* WT sample and a *KRAS* MT sample. **B,** Volcano plot as in **A**, but showing effect of *KRAS* mutation on Hallmark gene sets. The subset of the full set of 50 Hallmark gene sets with $P < 0.1$ is labeled.

consistently trend toward reduced infiltration in *KRAS* MT colorectal cancer (TCGA: $P = 0.09$; KFSYSCC: $P = 0.13$). To further characterize biological differences between *KRAS* MT and WT colorectal cancer, we compared the differences in expression of all 50 Hallmark gene sets (23). This revealed downregulation of multiple immune-related pathways within *KRAS* MT tumors across both datasets (Fig. 1B). In particular, we observed suppression of the IFNγ pathway in *KRAS* MT colorectal cancer in both datasets.

STAT1 and CXCL10 are downregulated in *KRAS* MT colorectal cancer

Given the disruption of the IFNγ pathway in *KRAS* MT colorectal cancer, we hypothesized that downstream genes would also be affected in these tumors. To test this, we examined the expression of the key IFNγ response gene, STAT1, at the mRNA level and at the protein level using digital IHC (Supplementary Fig. S2A–S2E). We found that *STAT1* mRNA expression was downregulated in *KRAS* MT colorectal cancer in both datasets (Supplementary Fig. S6). By performing IHC and then digitally segmenting tumors into epithelium, stromal, and background regions (Supplementary Fig. S1A and S1B), we found that the STAT1 protein was also downregulated in the epithelial compartment across a series of whole mount sections taken from 115 patients with primary colorectal cancer (RAS G12D/G13D MT $n = 28$, RAS non-G12D/G13D MT $n = 38$, RAS WT $n = 49$): STAT1 expression was reduced by RAS mutation whether samples were analyzed by H-scores ($P = 0.016$) or according to percentage of positive staining for STAT1 ($\chi^2 P = 0.033$; Table 1).

Table 1. IHC analysis

		Epithelium			Stroma		
		RAS MT	RAS WT	*P*	RAS MT	RAS WT	*P*
STAT1	Median H-score	180	238	0.016	88	122	0.086
	% H-score < 100	32.2	10.5	0.014	54.2	47.4	0.508
	% H-score > 200	40.7	60.5	0.056	13.6	23.7	0.200
CXCL10	Median H-score	93.5	108	0.080	24	24	0.858
	% H-score < 100	58.1	38.3	0.041	85.5	85.1	0.956
	% H-score > 200	8	23.4	0.025	4.8	2.1	0.558
Class II HLA	Median percentile score	125.2	136.8	0.260	143.9	135.8	0.051
	% Negative (0%–5%)	50.8	51.2	0.590	11.3	20.9	0.300
	% Positive (5%–50%)	42.9	37.2		87.1	79.1	
	% Strong (>50%)	6.4	11.6		1.6	0	

NOTE: Median histologic scores or percentile scores in epithelial and stromal regions. STAT1 and PD-L1 reactivity are represented by histologic scores. Class II HLA reactivity is represented by percentile scores. For median H and percentile scores, *P* values are derived with Mann–Whitney *U* test. For all other comparisons, *P* values are derived with χ^2 test.

We next asked whether STAT1 target molecules, CXCL10 and CIITA, were also dysregulated in *KRAS* MT tumors. We found that *CXCL10* was strongly downregulated in both datasets (Supplementary Fig. S6). This downregulation was confirmed at the protein level, with significantly more MT samples having H-scores <100 ($\chi^2P = 0.04$) and significantly more WT samples having H-scores >200 ($\chi^2P = 0.03$; Table 1). We also found that *CIITA* was downregulated in *KRAS* MT samples in the TCGA dataset (Supplementary Fig. S6). Although there was no such evidence for dysregulation of the mRNA in the KFSYSCC dataset (Supplementary Fig. S6), *CIITA* expression was generally low in this dataset (median *CIITA* expression below the fifth percentile). At the protein level, around 50% of both RAS MT and RAS WT colorectal cancer samples were completely negative for class II expression by IHC and only 6.4% RAS MT tumors had >50% class II–positive cells (Supplementary Figs. S1C and S1D and S2F–S2H; Table 1). When class II protein expression was analyzed in the cancer samples that had detectable expression of class II (i.e., excluding the class II negative cases in which transcriptional silencing of CIITA would prevent IFNγ inducibility via STAT1; refs. 30, 31), we found that RAS mutation was associated with reduced class II expression on the cancer cells (RAS MT class II–expressing colorectal cancer median epithelial class II H-score = 136.14, RAS WT median = 168.33, Mann–Whitney U $P = 0.01$) with no differences in stromal class II expression (RAS MT colorectal cancer stromal median = 146.96, RAS WT median = 141.56, Mann–Whitney U $P = 0.16$).

Reduced immune infiltration is independently associated with *KRAS* mutation and CMS subtype

Immune response in colorectal cancer has been reported to be suppressed in CMS2 (21). Hence, we hypothesized that the CIRC and other measures of immunity would be lowest in *KRAS* MT CMS2 tumors. We first confirmed that the CIRC was strongly suppressed in CMS2 relative to CMS1 and CMS4 in both the TCGA (Supplementary Fig. S7A; CMS2 vs. CMS1: two-tailed Wilcoxon rank sum $P = 1.2 \times 10^{-18}$; CMS2 vs. CMS4: $P = 5.5 \times 10^{-15}$) and KFSYSCC (Supplementary Fig. S7B; CMS2 vs. CMS1: $P = 1.1 \times 10^{-4}$; CMS2 vs. CMS4: $P = 9.0 \times 10^{-8}$) datasets. As expected, *KRAS* MT CMS2 samples had the lowest CIRC expression among all genotype × CMS subtype combinations in the TCGA dataset (Fig. 2A). These results were independently validated in the KFSYSCC dataset (Fig. 2B), although the consistent trends in relation to CMS3 did not reach significance. To determine whether *KRAS* mutation status and CMS classification are significantly and independently associated with immune infiltration, we performed a multivariate analysis of CIRC expression that included as parameters *KRAS* mutation status, CMS classification, primary tumor location, and, in the TCGA dataset where they were available, MSI status and neoantigen load. The analysis showed that *KRAS* MT and CMS2 (relative to CMS1 and CMS4) were independently predictive of reduced CIRC expression in the TCGA (Fig. 3A) and KFSYSCC (Fig. 3B) datasets. We next assessed whether *KRAS* mutation might have a CMS subtype-dependent effect. However, there was no evidence for a *KRAS* × CMS interaction in either dataset (TCGA: F test $P = 0.15$; KFSYSCC: $P = 0.67$). Finally, to delineate potential differential infiltration of specific subpopulations associated with *KRAS* MT CMS2 tumors, we examined the immune subpopulations most strongly associated with *KRAS* status (Fig. 1A) in the additional context of molecular subtype. We found that *KRAS* MT CMS2 tumors had reduced infiltration of cytotoxic cells relative to all other patient groups in the TCGA dataset (Fig. 4A), with a similar trend in the KFSYSCC dataset (Fig. 4B). *KRAS* MT CMS2 tumors also showed reduced infiltration of neutrophils and Th1 cells in both datasets relative to CMS1 and CMS4 patients, but not necessarily to *KRAS* WT CMS2 or (*KRAS* MT or WT) CMS3 patients.

Taken together, our results indicate that there is considerable heterogeneity within CMS subtypes, even when controlling for MSI status, and that this may be further dissected using *KRAS*

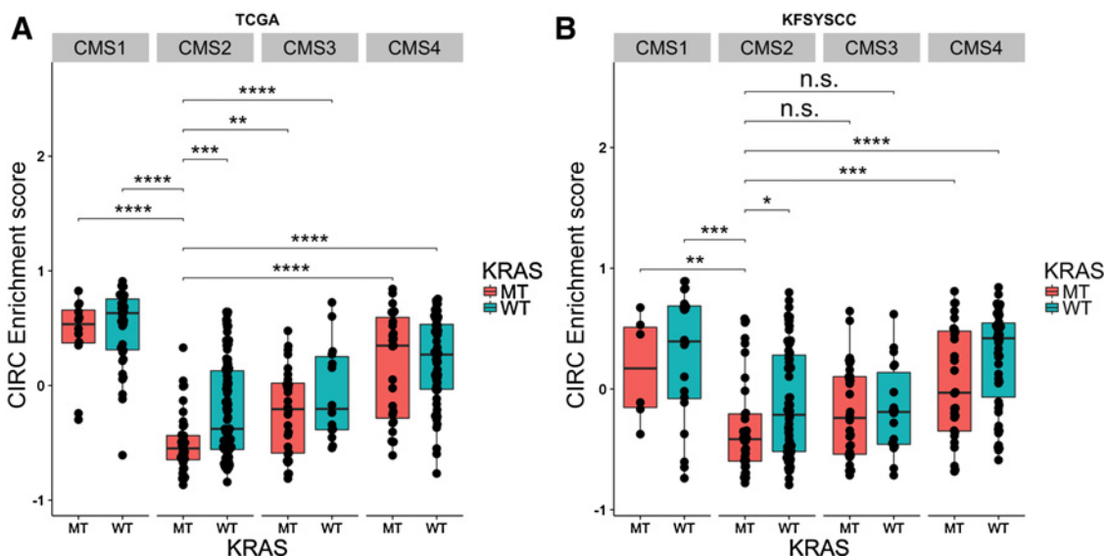

Figure 2.

CIRC expression is reduced in *KRAS*-mutant CMS2 tumors. Expression of CIRC versus CMS subtype and *KRAS* mutation status in TCGA (**A**; $n = 316$) or KFSYSCC (**B**; $n = 258$) datasets. n.s., not significant; *, $P < 0.05$; **, $P < 0.01$; ***, $P < 0.001$; ****, $P < 0.0001$; MT, mutation; WT, wild type.

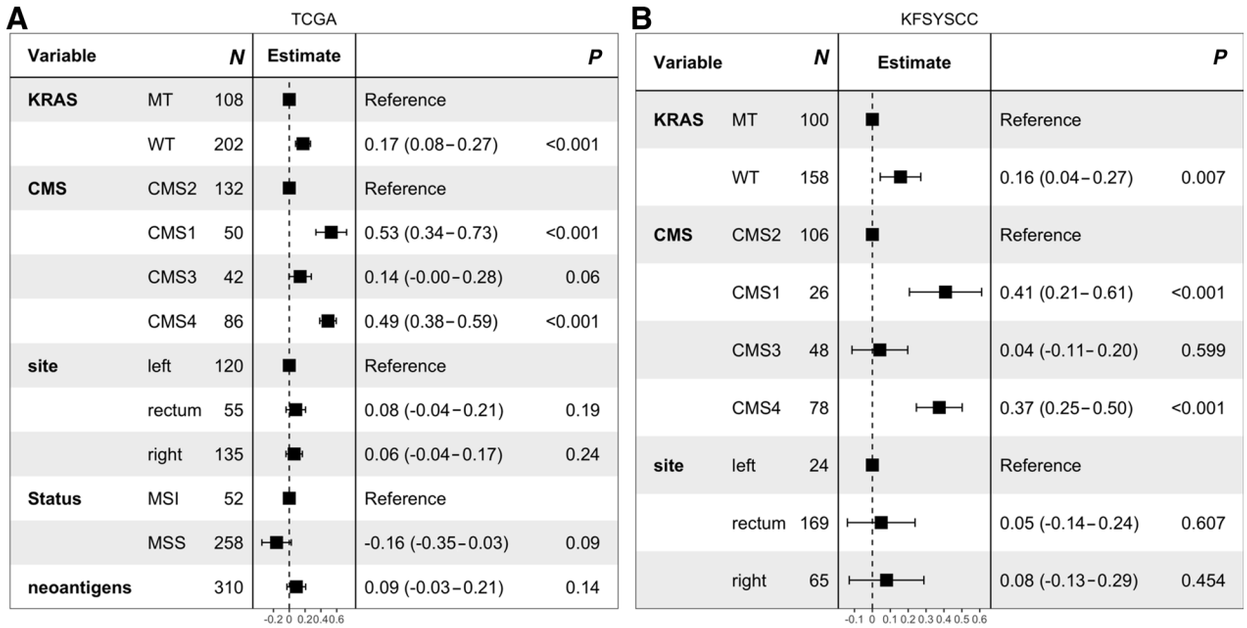

Figure 3.

CMS subtype and *KRAS* mutation are independently predictive of CIRC expression. Multivariate analysis performed across TCGA (**A**; $n = 310$) or KFSYSCC (**B**; $n = 258$) datasets.

mutation status. Although the data could not unambiguously resolve whether *KRAS* mutation has an effect specific to CMS2, the two factors are independently significant, that is, the level of immune infiltration and its characterization across immune cell subpopulations cannot be inferred without knowledge of both factors. The cumulative effect is such that *KRAS* MT CMS2 samples have reduced immune infiltration (of cytotoxic cells, neutrophils, and Th1 cells, as well as measured by the CIRC) relative to CMS1 or CMS4 samples harboring either MT or WT *KRAS*.

IFNγ pathway suppression is associated with both *KRAS* mutation and CMS subtype

To determine whether immune pathways downregulated in *KRAS* MT tumors (Fig. 1B) were additionally suppressed in CMS2 colorectal cancer, we evaluated the expression of these signatures in the context of *KRAS* mutation status and molecular classification. In the TCGA dataset, we found that *KRAS* MT CMS2 tumors exhibited reduced expression of all examined immune signatures (IFNγ, inflammatory response, IL6/JAK/STAT3 signaling, complement, and IFNα) relative to all patient groups (although the trend did not reach significance in relation to *KRAS* WT CMS2 when examining the IFNα pathway; Fig. 4C). These trends held in the KFSYSCC data set (Fig. 4D). In particular, *KRAS* MT CMS2 tumors showed significantly reduced expression of the IFNγ pathway relative to all other patient groups in both datasets, except relative to *KRAS* WT CMS2 in the KFSYSCC dataset, which nevertheless exhibited the same trend ($P = 0.05$).

Finally, we examined the IFNγ target gene STAT1, as well as its downstream targets, *CXCL10* and *CIITA*, to determine whether the previously observed association between the reduced expression of these three genes and *KRAS* mutation was independent of molecular subtype. First, we observed that, within CMS2, *KRAS* MT samples had lower expression of each of the genes relative to WT samples in both the TCGA ($P < 0.02$) and KFSYSCC ($P < 5.8 \times 10^{-3}$) datasets, with the exception of *CIITA* in the KFSYSCC dataset, as expected from its low expression in this dataset (Supplementary Fig. S8). Second, we performed multivariate analyses for all three genes in both datasets, excluding *CIITA* in the KFSYSCC dataset, which generally indicated that both *KRAS* mutation and CMS2 (relative to CMS1 and CMS4) were significantly and independently associated with reduced expression of the three genes. Specifically, *KRAS* mutation was significantly ($P < 1.1 \times 10^{-2}$) or marginally ($P = 0.05$ for *STAT1* in the TCGA dataset) associated with reduced gene expression, while CMS2 was associated with reduced gene expression relative to CMS1 ($P < 3.1 \times 10^{-3}$) and to CMS4 ($P < 1.2 \times 10^{-3}$, except for *STAT1* in the KFSYSCC dataset, where $P = 0.17$).

Discussion

We have previously shown that *KRAS* mutation is associated with reduced expression of the CIRC metagene, which summarizes 28 genes associated with innate and adaptive immunity. Here, we extend those earlier findings to: (i) explicitly characterize the nature of the suppressed immune infiltration, showing that *KRAS* MT tumors have reduced infiltration of cytotoxic cells and neutrophils (Fig. 1A); (ii) demonstrate that the IFNγ pathway is suppressed in *KRAS* MT tumors (Fig. 1B); (iii) demonstrate that KRAS mutation is associated with downregulation of STAT1 and CXCL10 at the mRNA (Supplementary Fig. S6) and protein (Table 1) levels; (iv) show that *KRAS* MT–associated immunosuppression is independent of CMS classification (Fig. 3; Supplementary Fig. S8); and (v) show that *KRAS* MT CMS2 colorectal cancer is significantly immunosuppressed relative to (*KRAS* MT or WT) CMS1 and CMS4 cancers and, based on several signatures in

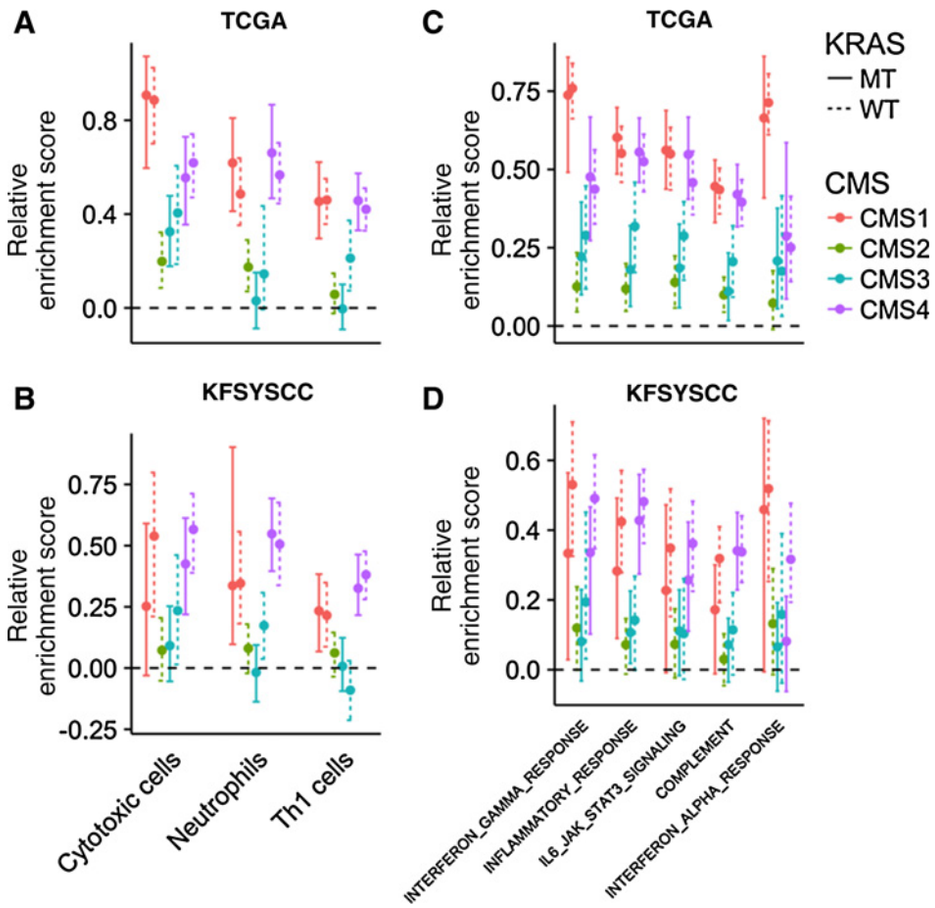

Figure 4.
KRAS MT CMS2 tumors are associated with reduced immune infiltration and downregulation of immune pathways. Enrichment score (*y*-axis) of immune populations (*x*-axis) of indicated *KRAS* x CMS subgroup relative to *KRAS* MT CMS2 subgroup in TCGA (**A**) and KFSYSCC (**B**) datasets. Relative enrichment is the Hodges–Lehmann estimator of the difference between the indicated subgroup and the *KRAS* MT CMS2 subgroup. Error bars represent 95% confidence intervals in estimator calculated using the method of Bauer (25). Enrichment relative to *KRAS* MT CMS2 subgroup of Hallmark immune pathways in TCGA (**C**) and KFSYSCC (**D**) datasets.

at least one of the two datasets, relative to *KRAS* WT CMS2 colorectal cancer as well (Figs. 2 and 4).

The *KRAS* MT–associated downregulation of the IFNγ pathway and reduced infiltration of cytotoxic T cells [i.e., those with properties common to $CD8^+$ T, Tγδ, and natural killer (NK) cells] and neutrophils indicate that the immunosuppressive impact of KRAS mutation that we previously observed is robust, if modest. Recent data demonstrate the interconnectedness of $CD8^+$ T cells and neutrophils with the IFNγ pathway in CRC (32): addition of neutrophils to $CD8^+$ T cells (activated via suboptimal concentrations of anti-CD3 and anti-CD28 antibodies) led to increased IFNγ release and T-cell proliferation. In turn, activated $CD8^+$ cells enhanced neutrophil viability. Furthermore, activated neutrophils colocalize with immature DCs, leading to their maturation (33). The resulting DCs drive T-cell proliferation and Th1 skewing.

Preclinically, RAS mutation has been shown to reduce the levels of STAT1 (17, 18). Consistent with these findings, we demonstrated that RAS MT cancers are associated with significantly lower STAT1 within the context of the tumor microenvironment. The preclinical data also showed that RAS mutation reduced STAT1-dependent transcriptional activity (17); indeed, we detected reduced expression of the STAT1 target CXCL10 at the RNA and protein levels in *KRAS* MT relative to WT samples. *KRAS* mutation may additionally downregulate CXCL10 via its activation of MEK–ERK signaling, which we observed in both datasets using a previously published (34) five-gene MEK signature (data not shown). We observed that *KRAS* MT reduced expression of a second STAT1 target, *CIITA*, in the TCGA dataset. No such trend was detected in the KFSYSCC dataset. However, *CIITA* expression was suppressed in this dataset, which would likely mask any *KRAS* MT–mediated STAT1 impact. Transcriptional repression of CIITA is seen in a proportion of colorectal cancer samples (30) as is the complete failure of IFNγ to induce class II expression in half of primary colorectal cancer cells (31). Both of these effects are RAS independent. To control for *CIITA* silencing (and thus lack of class II inducibilty), we analyzed the 50% of colorectal cancer samples that detectably expressed class II molecules (and in which *CIITA* must be transcribed and hence under the influence of STAT1). In these samples, we demonstrated that RAS MT cancers had significantly lower expression of class II surface makers compared with RAS WT cases. Significantly, we demonstrated that both CMS classification and *KRAS* mutation status are independently and significantly associated with dysregulation of *STAT1*, *CXCL10*, and *CIITA*. The CMS-associated effect presumably reflects previously reported reduced IFNγ signaling in CMS2 tumors (21), which leads to correspondingly reduced transcription of STAT1 target genes (17). Our findings and the cited literature are consistent with a cell-autonomous role for *KRAS* in modulating STAT1 and its downstream targets *CXCL10* and *CIITA*. Nevertheless, we cannot formally exclude the possibility that this *KRAS* effect is attributable, in whole or in part, to the reduced immune infiltration of CMS2 colorectal cancer with corresponding reduced environmental IFNγ. However these two factors are clearly intimately related.

Suppression of the CIRC was greatest in *KRAS* MT CMS2 samples. There may be a straightforward explanation for this phenomenon. CMS2 is the most Th1 immunosuppressed of the molecular subtypes with the lowest level of IFNγ signaling and thus lower levels of STAT1 and STAT1 target gene transcription. KRAS mutation shifts the IFNγ/STAT1 dose–response curve (17), such that for any level of IFNγ, there is less STAT1 transcription in a KRAS-mutated context. This effect is likely to be most biologically relevant where IFNγ levels are already limiting. The cumulative impact of low IFNγ (CMS2) and blunting of the IFNγ response (via mutant KRAS) may result in a level of STAT1-dependent promoter transcription that is insufficient to support robust and consistent expression of the critical downstream molecules. We considered the alternative explanation that the effect of KRAS mutation in CMS2 was due to it impacting the particular biology of CMS2. This subtype is characterized by high levels of Wnt and Myc signaling (21). Activation of Wnt/β-catenin signaling in melanoma reduces $CD8^+$ and IFNγ-producing $CD4^+$ cells, findings that have been generalized across other cancer types, including colorectal cancer (35), while MYC upregulation has been associated with reduced $CD4^+$ T-cell tumoral accumulation (36). *In vitro*, mutant RAS significantly enhances Wnt/β-catenin signaling in a mutant APC background and enhances downstream *MYC* transcription (37). Thus, we investigated whether KRAS mutation was deepening the Wnt and Myc drive in CMS2, and thus deepening immunosuppression via this mechanism. We found no robust, consistent evidence that *KRAS* mutation dysregulated the expression of the Wnt or Myc signatures within the context of CMS2 ($P > 0.07$ for comparisons of KRAS MT CMS2 vs. KRAS WT CMS2 for Wnt/β-catenin and Myc target gene sets).

As is the case for the majority of transcriptional and IHC analyses in colorectal cancer, our analysis was performed using primary resection samples. It is important to stress that the strength of Th1 immunity and class II expression in primary tissue are highly prognostic factors and are predictive of the presence of both synchronous metastatic disease and the development of subsequent metastases (38). Thus, understanding the independent impacts on the strength of Th1 immunity in primary tissue is of value in its own right. These results pose important questions for the larger body of immunotherapy trials that are instead directed at established metastatic or, in an adjuvant context, micrometastatic disease. Longitudinal expression studies following the evolution of disease progression should be undertaken to ascertain the concordance of CMS classification between primary and metastatic disease. However, existing data already suggest that immune cell densities ($CD8^+$, dendritic, and NK cells) are highly correlated between primary and metastatic colorectal cancer and between separate metastatic sites (39). Although it has been suggested that there is significant intratumoral heterogeneity of CMS, this analysis used separately macrodissected tissue from the center of the tumor and from the invasive front rather than bulk tumor (40). As was pointed out in the accompanying editorial, biopsy from the invasive margin will result in a large admixture of stromal cells not found in the center of the tumor, thus giving a CMS4-like signature and artificially introducing heterogeneity through selective sampling (41). Regardless of whether CMS or some other molecular subtypes prove to be pertinent to metastatic colorectal cancer, our results suggest that *KRAS* mutation is likely to modulate immune response within these subtypes: these data provide proof of principle that the immune status of RAS-mutant colorectal cancer is not homogenous across all colorectal cancer and that RAS mutation influences the immunobiology of molecularly defined colorectal cancer subtypes.

In summary, our results add a novel immunologic dimension to the growing appreciation of the biological heterogeneity of tumors harboring canonical mutations in colorectal cancer. The immunobiological status of RAS-mutant colorectal cancer varies according to transcriptional context, and the immunobiological status of CMS2 is dependent on RAS status. *KRAS* MT CMS2 appears to be a particularly immune-neglected group that will require therapy to initially activate a microenvironmental immune response if checkpoint blockade is considered in a combinatorial approach. RAS mutation itself may be a useful immunologic target in this group. Adoptive T-cell transfer of RAS MT-specific T cells has recently been shown to have therapeutic efficacy in colorectal cancer (42), and the use of T cells transduced with T-cell receptors recognizing RAS MT epitopes is also a potential therapy option (43). Our demonstration that a canonical mutation can be associated with widely differing expression of immune-related genes based on its transcriptional subtype may underlie some of the heterogeneity of responses seen with targeted therapies, although it is important to qualify this by acknowledging that our understanding of the transcriptional biology of metastatic disease is limited. In animal models, the activity of BRAF inhibitors is dependent on Th1 cell–mediated provision of CD40L and IFNγ (44). Similarly, the therapeutic effect of inactivation of oncogenic MYC is dependent upon $CD4^+$ cells (45). This suggests that the use of individual mutations as predictive biomarkers in colorectal cancer may be insufficient to predict the efficacy of targeted therapies without knowledge of the associated CMS subtype and its immune contexture. This hypothesis should be readily testable in the clinic.

Disclosure of Potential Conflicts of Interest

A.D. Beggs reports receiving other commercial research support from Illumina Inc. No potential conflicts of interest were disclosed by the other authors.

Authors' Contributions

Conception and design: N. Lal, O. Pickles, A.D. Beggs, B.E. Willcox, J. Guinney, G.W. Middleton

Development of methodology: N. Lal, G. Goussous, O. Pickles, A.D. Beggs, B.E. Willcox, J. Guinney

Acquisition of data (provided animals, acquired and managed patients, provided facilities, etc.): N. Lal, G. Goussous, O. Pickles, P. Taniere

Analysis and interpretation of data (e.g., statistical analysis, biostatistics, computational analysis): N. Lal, B.S. White, G. Goussous, M.J. Mason, B.E. Willcox, J. Guinney, G.W. Middleton

Writing, review, and/or revision of the manuscript: N. Lal, B.S. White, G. Goussous, O. Pickles, M.J. Mason, B.E. Willcox, J. Guinney, G.W. Middleton

Administrative, technical, or material support (i.e., reporting or organizing data, constructing databases): A.D. Beggs, J. Guinney

Study supervision: B.E. Willcox, J. Guinney, G.W. Middleton

Acknowledgments

B.S. White, M.J. Mason, and J. Guinney are grateful for the fruitful conversations with Drs. Benjamin Logsdon, Solveig Sieberts, and Rodrigo Dienstmann. N. Lal, G.W. Middleton, and B.E. Willcox gratefully acknowledge the contribution to this study made by Christopher Bagnall, the University of Birmingham's Digital Pathology Unit, and the Human Biomaterials Resource Centre, which has been supported through Birmingham Science City - Experimental Medicine Network of Excellence project. We would like to thank University of Birmingham Alumni for funding the automated staining platform. N. Lal and O. Pickles

were supported by Cancer Research UK clinical PhD studentships. B.E. Willcox was supported by a Wellcome Trust investigator award. IHC costs and software were supported by a Birmingham Experimental Cancer Medicine Centre (ECMC) research programme (principal investigators: G.W. Middleton and B.E. Willcox).

A.D. Beggs acknowledges funding from the Wellcome Trust (102732/Z/13/Z), Cancer Research UK (C31641/A23923), and the Medical Research Council (MR/M016587/1).

The costs of publication of this article were defrayed in part by the payment of page charges. This article must therefore be hereby marked *advertisement* in accordance with 18 U.S.C. Section 1734 solely to indicate this fact.

Received April 20, 2017; revised August 22, 2017; accepted October 17, 2017; published OnlineFirst October 23, 2017.

References

1. Galon J. Type, density, and location of immune cells within human colorectal tumors predict clinical outcome. Science 2006;313:1960–4.
2. Ossendorp F, Mengede E, Camps M, Filius R, Melief CJ. Specific T helper cell requirement for optimal induction of cytotoxic T lymphocytes against major histocompatibility complex class II negative tumors. J Exp Med 1998;187:693–702.
3. Becht E, Giraldo NA, Dieu-Nosjean MC, Sautes-Fridman C, Fridman WH. Cancer immune contexture and immunotherapy. Curr Opin Immunol 2016;39:7–13.
4. Ridge JP, Di Rosa F, Matzinger P. A conditioned dendritic cell can be a temporal bridge between a CD4+ T-helper and a T-killer cell. Nature 1998;393:474–8.
5. Bos R, Sherman LA. CD4+ T-cell help in the tumor milieu is required for recruitment and cytolytic function of CD8+ T lymphocytes. Cancer Res 2010;70:8368–77.
6. Quezada SA, Simpson TR, Peggs KS, Merghoub T, Vider J, Fan X, et al. Tumor-reactive CD4(+) T cells develop cytotoxic activity and eradicate large established melanoma after transfer into lymphopenic hosts. J Exp Med 2010;207:637–50.
7. Kreiter S, Vormehr M, van de Roemer N, Diken M, Löwer M, Diekmann J, et al. Mutant MHC class II epitopes drive therapeutic immune responses to cancer. Nature 2015;520:692–6.
8. Topalian SL, Drake CG, Pardoll DM. Immune checkpoint blockade: a common denominator approach to cancer therapy. Cancer Cell 2015;27:450–61.
9. Le DT, Uram JN, Wang H, Bartlett BR, Kemberling H, Eyring AD, et al. PD-1 blockade in tumors with mismatch-repair deficiency. N Engl J Med 2015;372:2509–20.
10. Giannakis M, Mu XJ, Shukla SA, Qian ZR, Cohen O, Nishihara R, et al. Genomic correlates of immune-cell infiltrates in colorectal carcinoma. Cell Rep 2016 Apr 14. [Epub ahead of print].
11. Johnson DB, Estrada MV, Salgado R, Sanchez V, Doxie DB, Opalenik SR, et al. Melanoma-specific MHC-II expression represents a tumour-autonomous phenotype and predicts response to anti-PD-1/PD-L1 therapy. Nat Commun 2016;7:10582.
12. Yan H, Hou X, Li T, Zhao L, Yuan X, Fu H, et al. CD4+ T cell-mediated cytotoxicity eliminates primary tumor cells in metastatic melanoma through high MHC class II expression and can be enhanced by inhibitory receptor blockade. Tumour Biol 2016 Oct 5. [Epub ahead of print].
13. Muhlethaler-Mottet A, Di Berardino W, Otten LA, Mach B. Activation of the MHC class II transactivator CIITA by interferon-gamma requires cooperative interaction between Stat1 and USF-1. Immunity 1998; 8:157–66.
14. Kaplan DH, Shankaran V, Dighe AS, Stockert E, Aguet M, Old LJ, et al. Demonstration of an interferon gamma-dependent tumor surveillance system in immunocompetent mice. Proc Natl Acad Sci U S A 1998;95: 7556–61.
15. Gangur V, Simons FE, Hayglass KT. Human IP-10 selectively promotes dominance of polyclonally activated and environmental antigen-driven IFN-gamma over IL-4 responses. FASEB J 1998;12:705–13.
16. Mikhak Z, Fleming CM, Medoff BD, Thomas SY, Tager AM, Campanella GS, et al. STAT1 in peripheral tissue differentially regulates homing of antigen-specific Th1 and Th2 cells. J Immunol 2006;176: 4959–67.
17. Klampfer L, Huang J, Corner G, Mariadason J, Arango D, Sasazuki T, et al. Oncogenic Ki-ras inhibits the expression of interferon-responsive genes through inhibition of STAT1 and STAT2 expression. J Biol Chem 2003; 278:46278–87.
18. Klampfer L, Huang J, Shirasawa S, Sasazuki T, Augenlicht L. Histone deacetylase inhibitors induce cell death selectively in cells that harbor activated kRasV12: The role of signal transducers and activators of transcription 1 and p21. Cancer Res 2007;67:8477–85.
19. Maudsley DJ, Bateman WJ, Morris AG. Reduced stimulation of helper T cells by Ki-ras transformed cells. Immunology 1991;72:277–81.
20. Lal N, Beggs AD, Willcox BE, Middleton GW. An immunogenomic stratification of colorectal cancer: Implications for development of targeted immunotherapy. OncoImmunology 2015;4:e976052.
21. Guinney J, Dienstmann R, Wang X, de Reynies A, Schlicker A, Soneson C, et al. The consensus molecular subtypes of colorectal cancer. Nat Med 2015;21:1350–6.
22. Bindea G, Mlecnik B, Tosolini M, Kirilovsky A, Waldner M, Obenauf Anna C, et al. Spatiotemporal dynamics of intratumoral immune cells reveal the immune landscape in human cancer. Immunity 2013;39: 782–95.
23. Liberzon A, Birger C, Thorvaldsdottir H, Ghandi M, Mesirov JP, Tamayo P. The Molecular Signatures Database (MSigDB) hallmark gene set collection. Cell Syst 2015;1:417–25.
24. Hanzelmann S, Castelo R, Guinney J. GSVA: gene set variation analysis for microarray and RNA-seq data. BMC Bioinformatics 2013;14:7.
25. Bauer DF. Constructing confidence sets using rank statistics. J Am Stat Assoc 1972;67:687–90.
26. Charoentong P, Finotello F, Angelova M, Mayer C, Efremova M, Rieder D, et al. Pan-cancer immunogenomic analyses reveal genotype-immunophenotype relationships and predictors of response to checkpoint blockade. Cell Rep 2017;18:248–62.
27. Derry JM, Mangravite LM, Suver C, Furia MD, Henderson D, Schildwachter X, et al. Developing predictive molecular maps of human disease through community-based modeling. Nat Genet 2012; 44:127–30.
28. Løvig T, Andersen SN, Thorstensen L, Diep CB, Meling GI, Lothe RA, et al. Strong HLA-DR expression in microsatellite stable carcinomas of the large bowel is associated with good prognosis. Br J Cancer 2002;87: 756–62.
29. Guinney J, Ferte C, Dry J, McEwen R, Manceau G, Kao KJ, et al. Modeling RAS phenotype in colorectal cancer uncovers novel molecular traits of RAS dependency and improves prediction of response to targeted agents in patients. Clin Cancer Res 2014;20:265–72.
30. Satoh A, Toyota M, Ikeda H, Morimoto Y, Akino K, Mita H, et al. Epigenetic inactivation of class II transactivator (CIITA) is associated with the absence of interferon-gamma-induced HLA-DR expression in colorectal and gastric cancer cells. Oncogene 2004;23:8876–86.
31. Stoneman V, Morris A. Induction of intercellular adhesion molecule 1 and class II histocompatibility antigens in colorectal tumour cells expressing activated ras oncogene. Clin Mol Pathol 1995;48:M326–32.
32. Governa V, Trella E, Mele V, Tornillo L, Amicarella F, Cremonesi E, et al. The interplay between neutrophils and CD8+ T cells improves survival in human colorectal cancer. Clin Cancer Res 2017;23:3847–58.
33. van Gisbergen KP, Sanchez-Hernandez M, Geijtenbeek TB, van Kooyk Y. Neutrophils mediate immune modulation of dendritic cells through glycosylation-dependent interactions between Mac-1 and DC-SIGN. J Exp Med 2005;201:1281–92.
34. Dry JR, Pavey S, Pratilas CA, Harbron C, Runswick S, Hodgson D, et al. Transcriptional pathway signatures predict MEK addiction and response to selumetinib (AZD6244). Cancer Res 2010;70:2264–73.
35. Luke JJ, Bao R, Spranger S, Sweis RF, Gajewski TF. Correlation of WNT/β-catenin pathway activation with immune exclusion across most human cancers. J Clin Oncol 34:15s, 2016(suppl; abstr 3004).

36. Casey SC, Tong L, Li Y, Do R, Walz S, Fitzgerald KN, et al. MYC regulates the antitumor immune response through CD47 and PD-L1. Science 2016; 352:227–31.
37. Janssen KP, Alberici P, Fsihi H, Gaspar C, Breukel C, Franken P, et al. APC and oncogenic KRAS are synergistic in enhancing Wnt signaling in intestinal tumor formation and progression. Gastroenterology 2006;131: 1096–109.
38. Mlecnik B, Bindea G, Kirilovsky A, Angell HK, Obenauf AC, Tosolini M, et al. The tumor microenvironment and Immunoscore are critical determinants of dissemination to distant metastasis. Sci Transl Med 2016; 8:327ra26.
39. Remark R, Alifano M, Cremer I, Lupo A, Dieu-Nosjean MC, Riquet M, et al. Characteristics and clinical impacts of the immune environments in colorectal and renal cell carcinoma lung metastases: influence of tumor origin. Clin Cancer Res 2013;19:4079–91.
40. Dunne PD, McArt DG, Bradley CA, O'Reilly PG, Barrett HL, Cummins R, et al. Challenging the cancer molecular stratification dogma: intratumoral heterogeneity undermines consensus molecular subtypes and potential diagnostic value in colorectal cancer. Clin Cancer Res 2016; 22:4095–104.
41. Morris JS, Kopetz S. Tumor microenvironment in gene signatures: critical biology or confounding noise? Clin Cancer Res 2016;22:3989–91.
42. Tran E, Robbins PF, Lu YC, Prickett TD, Gartner JJ, Jia L, et al. T-cell transfer therapy targeting mutant KRAS in cancer. N Engl J Med 2016;375:2255–62.
43. Wang QJ, Yu Z, Griffith K, Hanada K, Restifo NP, Yang JC. Identification of T-cell receptors targeting KRAS-mutated human tumors. Cancer Immunol Res 2016;4:204–14.
44. Ho PC, Meeth KM, Tsui YC, Srivastava B, Bosenberg MW, Kaech SM. Immune-based antitumor effects of BRAF inhibitors rely on signaling by CD40L and IFNgamma. Cancer Res 2014;74:3205–17.
45. Rakhra K, Bachireddy P, Zabuawala T, Zeiser R, Xu L, Kopelman A, et al. CD4(+) T cells contribute to the remodeling of the microenvironment required for sustained tumor regression upon oncogene inactivation. Cancer Cell 2010;18:485–98.